

A New Gain Calibration and Background Filter for the *Chandra* LETG/HRC-S Spectrometer

Bradford J. Wargelin and Peter W. Ratzlaff
Harvard-Smithsonian Center for Astrophysics/CXC

Abstract

The gain of *Chandra*'s HRC-S detector has decreased significantly over the past 20 years, by around a factor of four in some areas. Although the HRC-S has very little energy resolution (median pulse height changes by less than 10% for a factor of two change in X-ray energy), it has enough that an accurate gain calibration allows around half of the background signal (after standard Level-2 pipeline processing) to be filtered out with only about 1% loss of valid X-ray events.

We describe our analysis of nearly 100 LETG/HRC-S observations of bright sources (HZ 43 for long wavelengths, Mkn 421 and PKS 2155 for short, and three novae for intermediate wavelengths) to measure the temporal and spatial dependence of the HRC-S gain on scales of 80 pixels along the LETG dispersion axis (about 0.6 Å). We include corrections for the effects of spectral contamination by higher-order diffraction, and also utilize 30 short grating-less observations of HZ43 to map gain in areas where gain losses are especially large and/or grating spectra are faint.

1. Introduction

The purpose of a gain map is to obtain, for any given X-ray energy, identical pulse height distributions (PHDs) from all areas of the detector at all times. As seen in Fig. 1, the gain of the HRC-S varies significantly across the detector, and has also changed over time, with calibration updates in 2001 and 2008. The 2008 calibration was rescaled in 2012 following an increase in detector high voltage that (temporarily) restored the HRC-S gain and QE. A new calibration was begun in 2017, which revealed that the two-parameter gain equation adopted in 2008 was not well suited for very low gains, and analysis was restarted in 2019 to use one-parameter rescaling. The new gain calibration and associated background filter will be available in early 2020.

A note on nomenclature: Coarse positions in the HRC-S are given by coordinates CRSU (short axis) and CRSV (dispersion axis), which increment by 1 for each 'tap'. Each tap corresponds to a group of position signal readouts, which is digitized into 256 × 256 pixels.

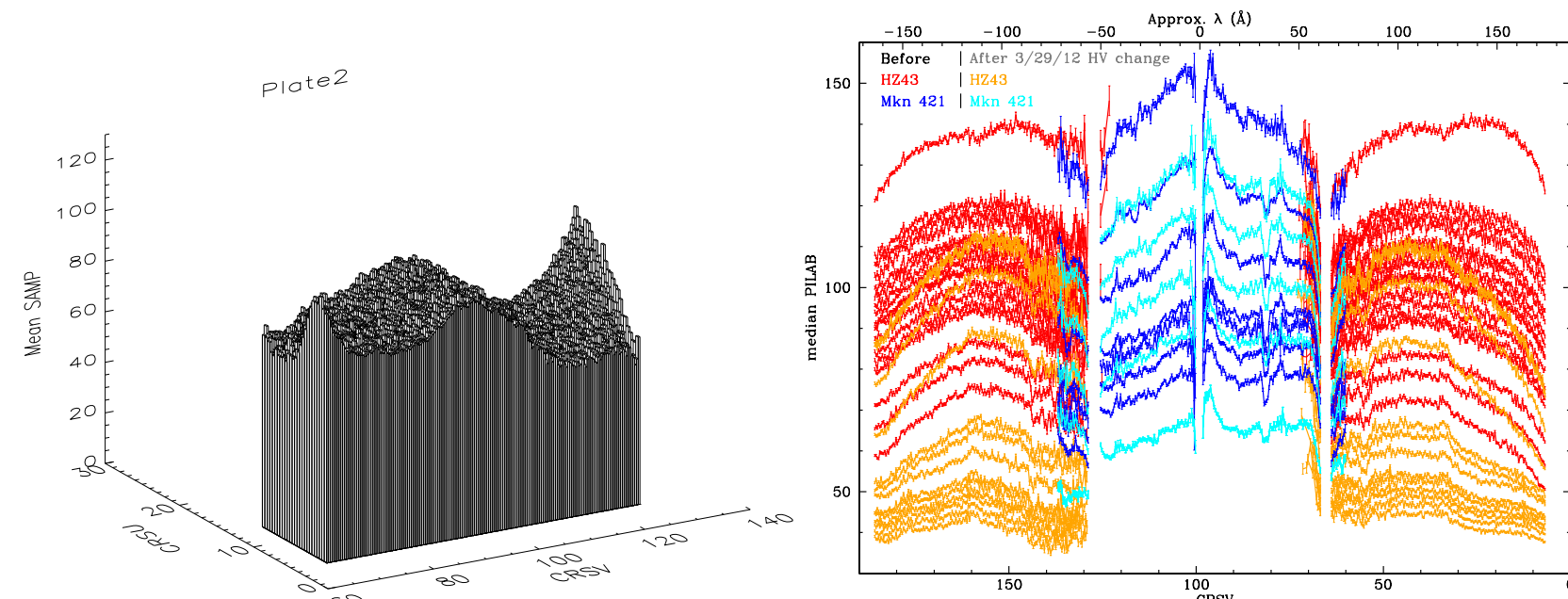


Figure 1: Left: Mean pulse height (SAMP) on the center plate, from pre-flight flat field illumination with C-K (277 eV) X rays. Right: PHD median after applying spatial gain corrections from lab calibration. As discussed in Section "Spatial Adjustments," the fully corrected curves should vary smoothly and monotonically with λ , without small scale jumps (e.g., CRSV=82), or larger scale dips near plate ends.

2. Improvements Over 2008 Methodology

In addition to having more observational data available, the new analysis benefits from a number of improvements over previous work, including:

- Spectral extraction regions optimized to reduce background contamination
- Stricter exclusion of periods of enhanced background
- End-to-end analysis on spatial scale of 1/3 tap (along dispersion axis)
- More accurate corrections for higher-order spectral contamination
- Reconciling gains across plate gaps using constant-spectrum data from 30 short off-axis no-grating HZ 43 observations.

3. Flight Data Selection

Gain changes during flight are calibrated by measuring PHDs over time (primarily characterized by the median of the PHD), using data from frequently observed continuum sources. HZ 43 (white dwarf) covers longer wavelengths, mostly on the two outer plates. PKS 2155 and Mkn 421 (blazars) cover shorter wavelengths, mostly on the inner plate. Calibration around the plate gaps has larger uncertainties because emission from all three sources is relatively weak at those wavelengths (~50-70 Å), and because of higher order contamination in the short-wavelength spectra. An additional eight observations from bright novae collectively cover from 14 to ~55 Å, and results from their pure 1st-order spectra are used to fine-tune the higher-order corrections for Mkn 421 and PKS 2155.

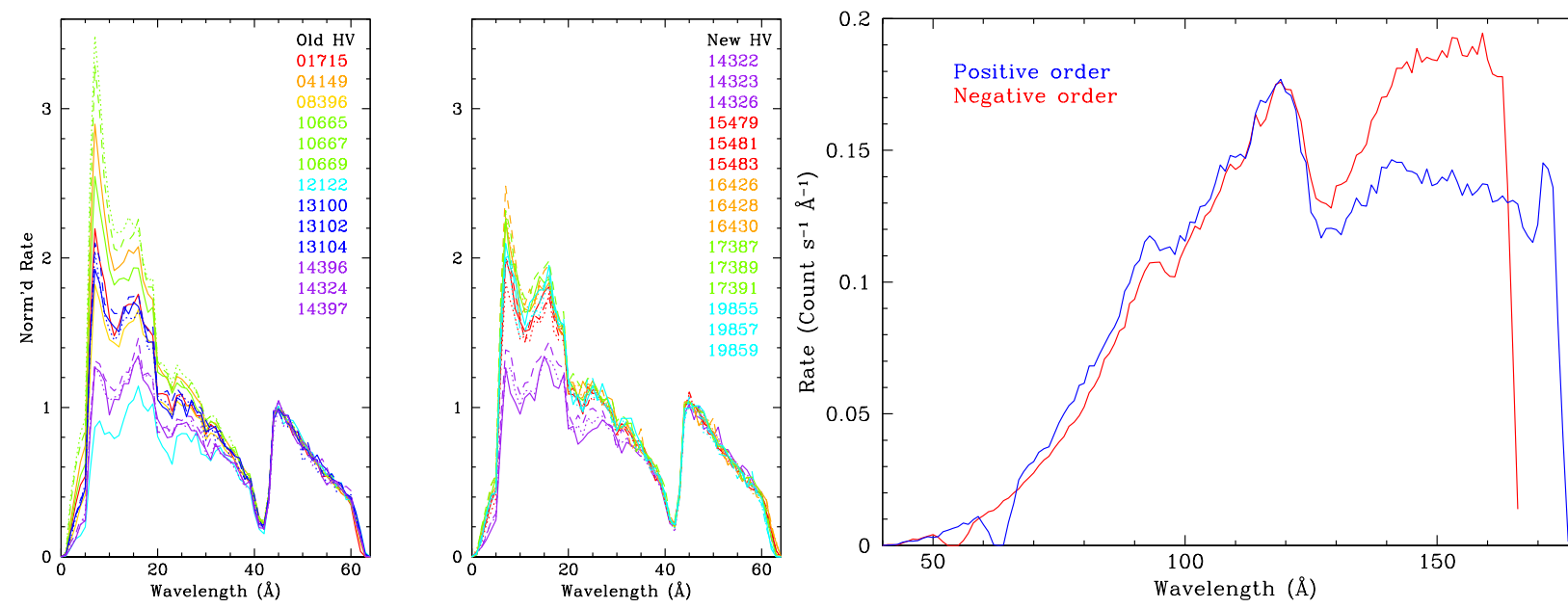


Figure 2: Left: Mkn 421 spectra normalized to rates at 45 Å, showing spectral shape variations. Rates near 6 Å range from 0.03 to 0.6 ct/s/Å. PKS 2155 spectra are similar, usually with lower rates. Right: HZ 43 spectrum, which is unvarying.

4. Higher Order Contamination

As noted earlier, higher orders contribute significantly to the spectra of Mkn 421 and PKS 2155 at all but the shortest wavelengths. Because of the (small) energy sensitivity of the HRC-S (Fig. 3Left), this shifts the net PHD toward higher channels than for a pure 1st-order spectrum.

To correct for this effect, we compute the flux contribution of orders $m = 1 - 12$ at each position (in detector coordinates) along the dispersed spectrum while taking into account the $\pm 20''$ source dither, create a net PHD from the weighted sum of the PHDs for each order (constructed from PHDs of pure 1st order spectra), and measure the medians of the summed and pure 1st order PHDs. Their ratio is then the correction factor. Fig. 3Right illustrates the contribution of higher orders in an example observation and their effect on the measured PHD.

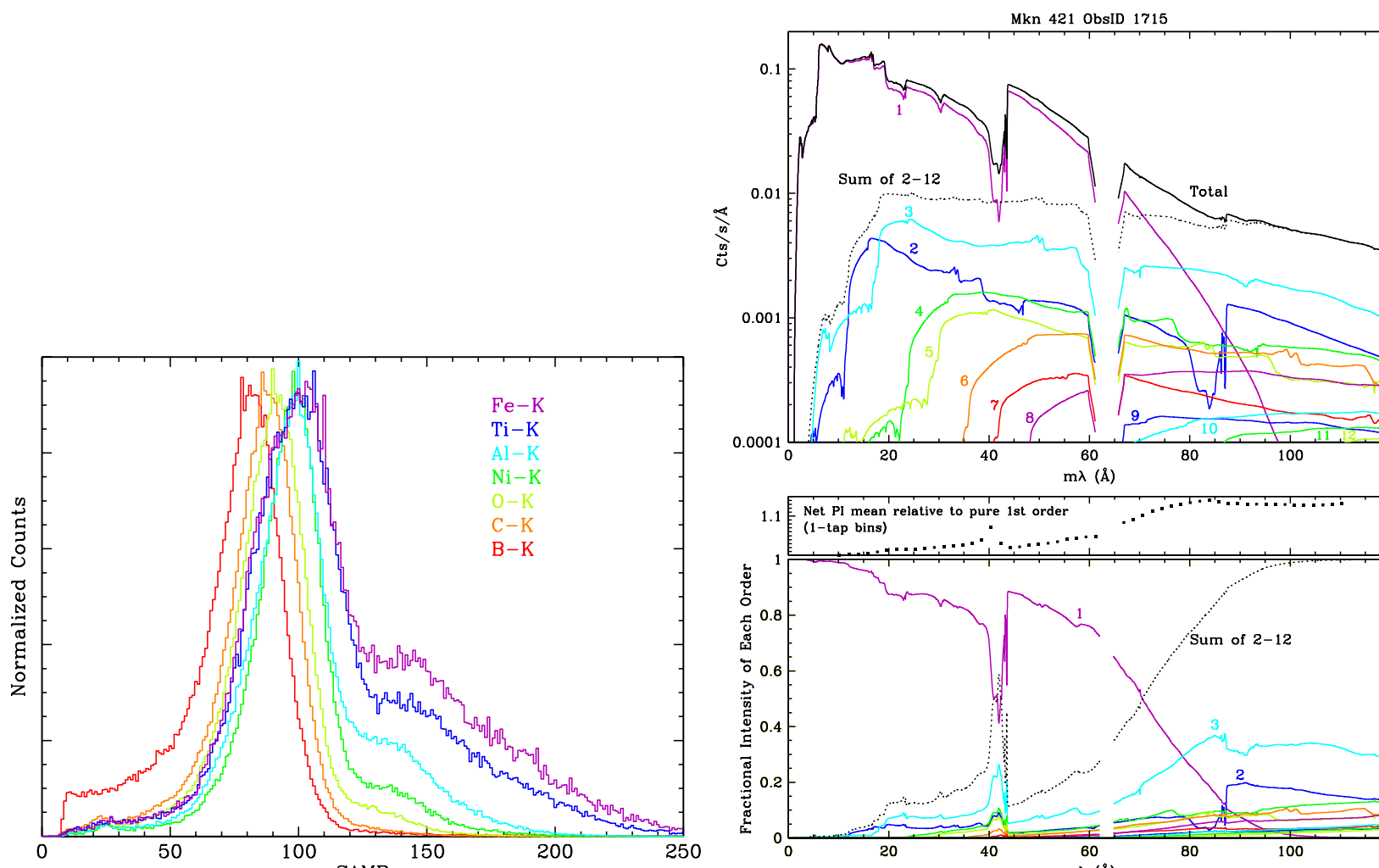


Figure 3: Left: PHDs from lab calibration, illustrating their energy dependence. Right: Relative fluxes from orders $m = 1 - 12$ of a Mkn 421 observation. The thin middle panel shows the net shift in PHD mean as a function of wavelength. (These and subsequent figures usually show results from earlier analyses; the current analysis is more accurate and detailed, but incomplete.)

5. Time Dependence

Once the PHD medians for each subtap along the dispersion axis have been measured, and if necessary corrected for higher orders, their time dependence can be fitted. A sum of exponential and linear decay works well, with separate fits for data before and after the early-2012 detector voltage change. Fig. 4 shows such data from Plate1 of the detector (CRSV=6-63). The fits are then used to create two Calibration DataBase (CALDB) files with 18 epochs, for before and after the 2012 HV change.

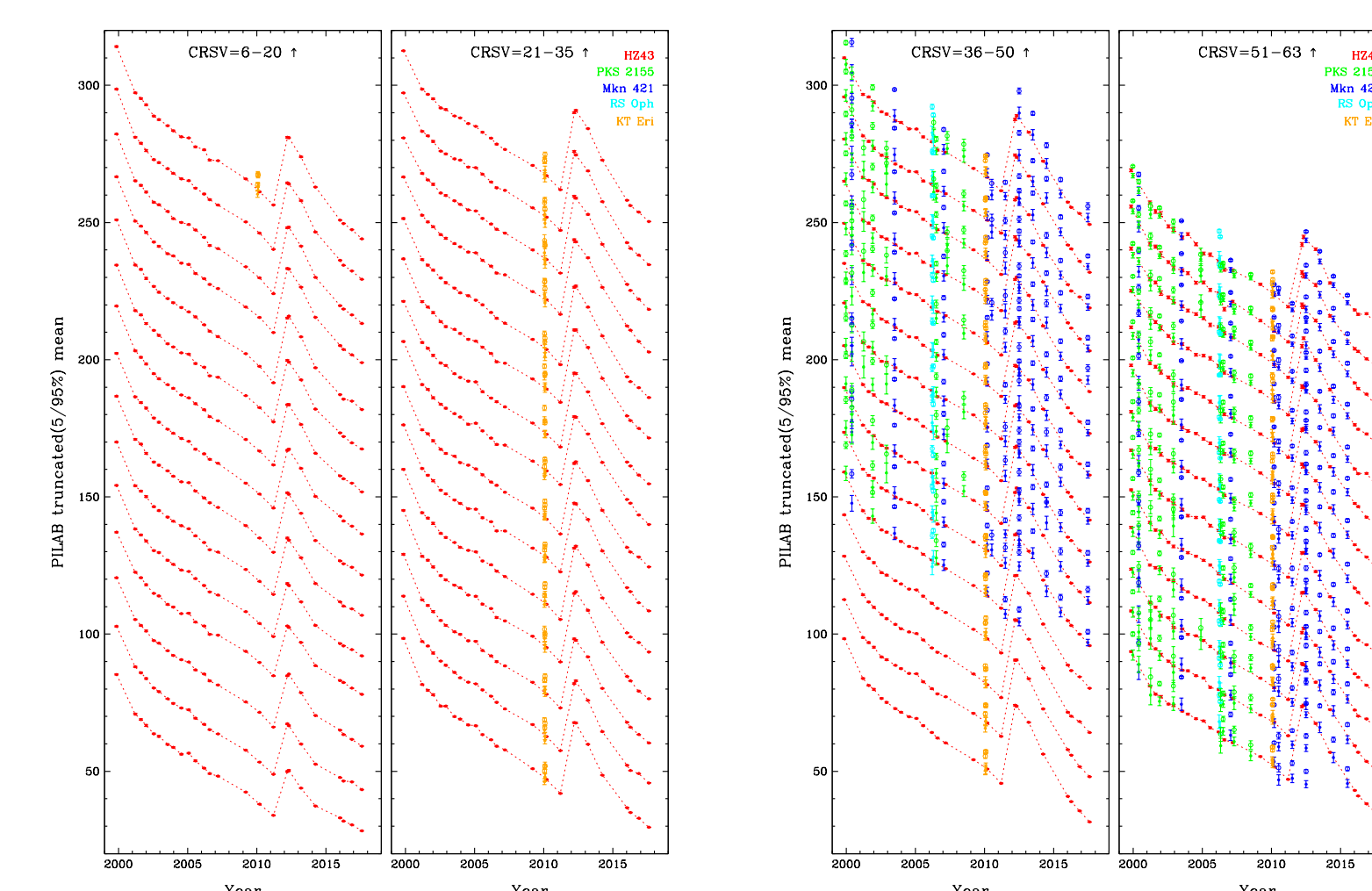


Figure 4: PHD means as a function of time, in 1-tap bins, before (open circles) and after (solid) corrections for higher order contamination. (The current analysis uses medians, and 1/3-tap bins.)

6. Spatial Adjustments

Even after the lab and time-dependence corrections, the gain map is not complete, because position-dependent gain changes occur between the time of lab calibration and flight. Unfortunately, there is no way to directly tie the monoenergetic flat field lab exposures to on-orbit dispersed spectra, except at a few isolated points.

We can, however, use an LETG/HRC-S observation of HZ43 made 10' off axis (ObsID 1170) to guide the overall shape of the median PI vs. λ relationship by requiring that on- and off-axis curves match as a function of λ despite the differences in their corresponding positions on the detector.

We have also made 30 observations of HZ43 without the LETG (see Fig. 5), sampling detector response to a fixed source spectrum from many points along the HRC-S, particularly near the plate gaps where calibration is difficult because of weak astrophysical spectra, and spatial gain variations tend to be large (Fig. 6Left).

Lastly, we require that PHD medians vary smoothly as a function of wavelength, using summed PHDs from all the calibration observations that have been corrected for the gain's time dependence to obtain excellent statistical quality, yielding very precise subtap-to-subtap gain adjustments.



Figure 5: Image of merged data (dithered, in detector coordinates) from a set of 14 off-axis no-grating observations of HZ43, used to measure relative gain near/across the HRC-S plate gaps.

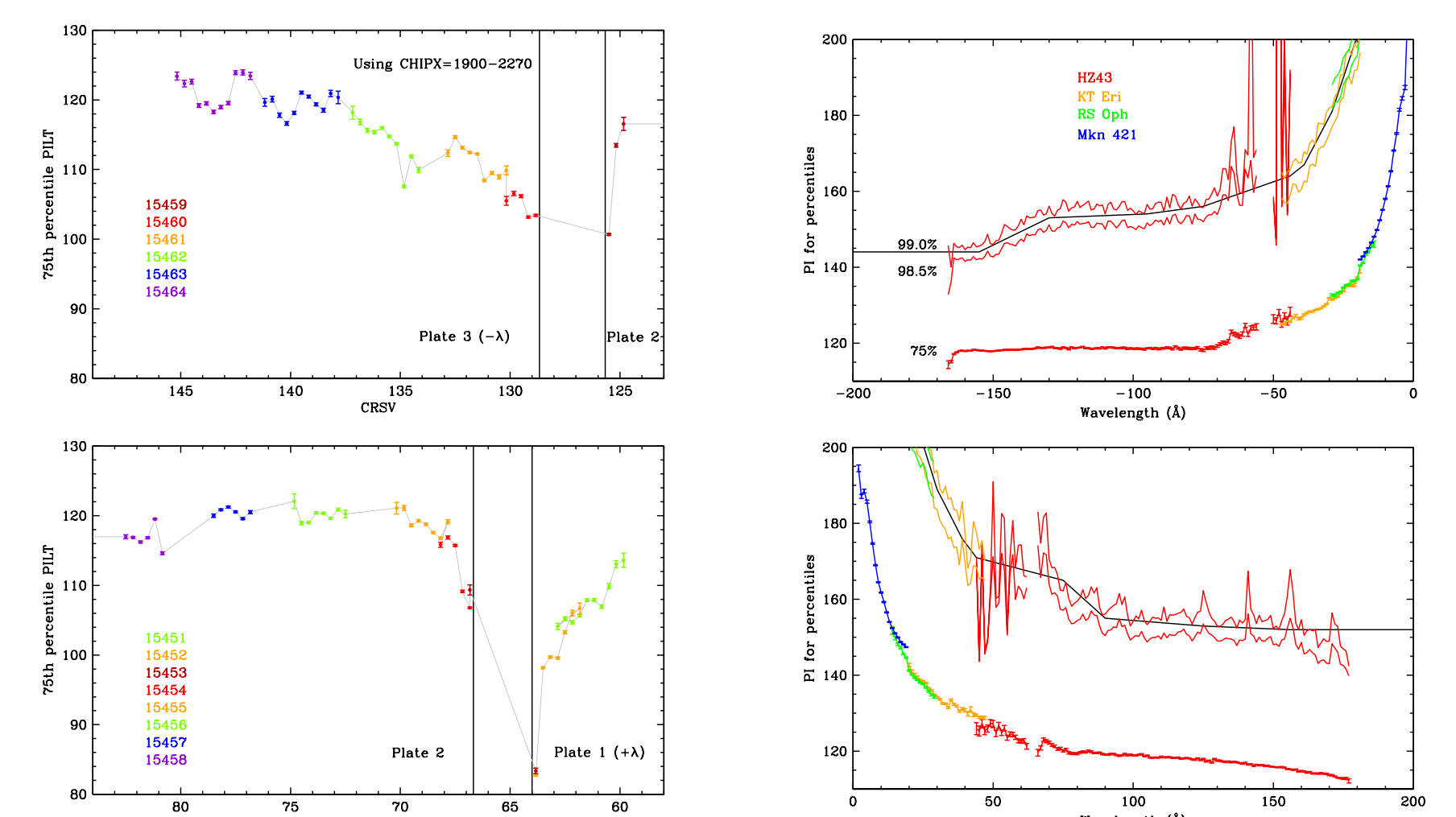


Figure 6: Left: 75th percentile PHD channels, by CRSV subtap, of data from Fig. 5 after application of time-dependence and lab-based spatial gain corrections. With a uniform source spectrum, a complete gain calibration would yield the same value at all points; these results illustrate that there are additional gain changes between the time of lab calibration and on-orbit observations. Right: PHD metrics from merged on-orbit spectra after applying gain corrections derived from the results in the Left figure and other analyses. The 75th percentile metrics now vary smoothly and monotonically with wavelength.

7. Background Filter

Once all the temporal and spatial gain corrections have been defined, they are applied to the summed observational calibration data, yielding precise measurements of PHD metrics at high percentiles as a function of wavelength (see Fig. 6Right). From those results we create a PI vs. λ filter that removes roughly half of the detector background in LETG/HRC-S spectra that remains after Level 2 processing, while discarding only 1.0-1.5% of X-ray events.

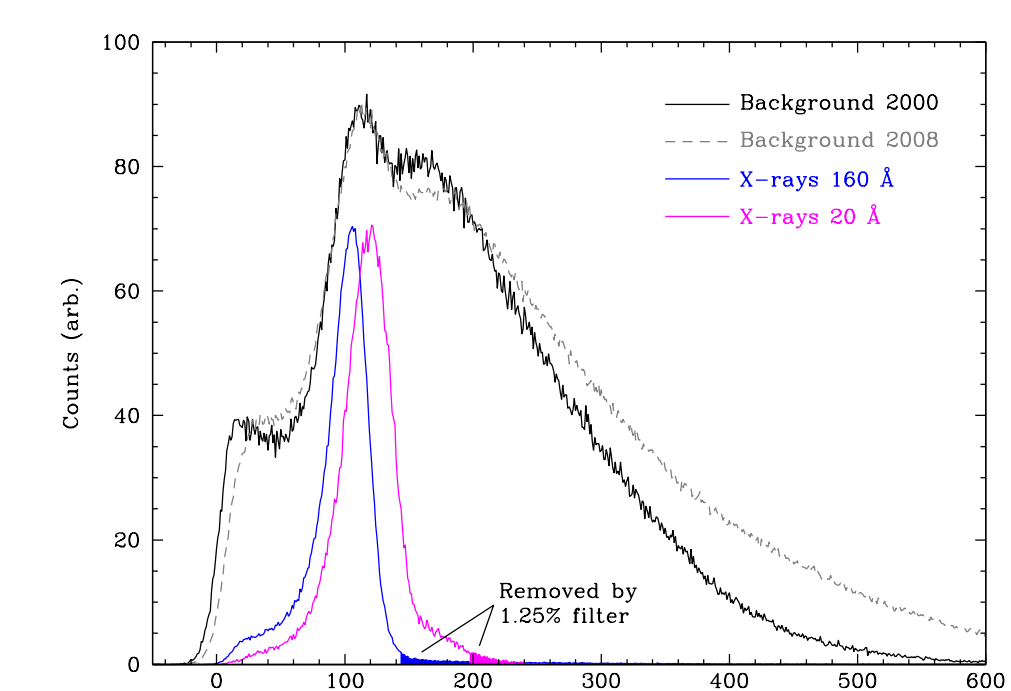


Figure 7: PHDs for flight background in 2000 and 2008, and for X-rays at 20 and 160 Å. The difference between background and X-ray PHDs is the basis of the pulse-height filter, which removes roughly half of the Level 2 background over most of the LETG wavelength range.